Effect of exportin 1/XPO1 nuclear export pathway inhibition on coronavirus replication.

Masmudur M. Rahman[1 4 5 #], Bereket Estifanos[2 4], Honor L. Glenn[2], Ami D. Gutierrez-Jensen[1], Karen Kibler[3], Yize Li[3 5], Bertram Jacobs[3 5], Grant McFadden[5], Brenda G. Hogue[2 4 5 #]

1 Center for Personalized Diagnostics, Biodesign Institute, Arizona State University, Tempe, AZ 85287, USA.

2 Center for Applied Structural Discovery, Biodesign Institute, Arizona State University, Tempe, AZ 85287, USA.

3 Center for ASU-Banner Neurodegenerative Disease Research Center, Biodesign Institute, Arizona State University, Tempe, AZ 85287, USA.

4 School of Life Sciences Microbiology Graduate Program, Arizona State University, Tempe, AZ 85287, USA

5 School of Life Sciences, Arizona State University, Tempe, AZ 85287, USA

Corresponding authors:

Masmudur M. Rahman: masmudur.rahman@asu.edu

Brenda G. Hogue: brenda.hogue@asu.edu

Abstract

Nucleocytoplasmic transport of proteins using XPO1 (exportin 1) plays a vital role in cell proliferation and survival. Many viruses also exploit this pathway to promote infection and replication. Thus, inhibiting the XPO1-mediated nuclear export pathway with selective inhibitors has a diverse effect on virus replication by regulating antiviral, proviral, and anti-inflammatory pathways. The XPO1 inhibitor, Selinexor, is an FDA-approved anticancer drug predicted to have antiviral or proviral functions against viruses. Here, we observed that pretreatment of cultured cell lines from human or mouse origin with nuclear export inhibitor Selinexor significantly enhanced protein expression and replication of Mouse Hepatitis Virus (MHV), a mouse coronavirus. Knockdown of cellular XPO1 protein expression also significantly enhanced the replication of MHV in human cells. However, for SARS-CoV-2, selinexor treatment had diverse effects on virus replication in different cell lines. These results indicate that XPO1-mediated nuclear export pathway inhibition might affect coronavirus replication depending on cell types and virus origin.

44 **Introduction**

45 The nucleocytoplasmic transport of proteins and other molecules is a highly regulated cellular
46 process. Many nuclear export (called exportins) and import (called importins) proteins are
47 involved in this process by exploiting nuclear pore complexes that form proteinaceous channels
48 in the nuclear envelope (1, 2). Exportin 1 (XPO1), also known as CRM1 (chromosome region
49 maintenance 1), is one of the major nuclear export proteins, transporting hundreds of cellular
50 cargo proteins involved in diverse cellular processes such as transcription, translation, cellular
51 growth, differentiation, and mediating inflammatory responses that include antiviral pathways (3,
52 4). Thus, direct inhibition of XPO1 function has been explored as a potential antiviral and
53 anticancer therapeutic target (5-8). Various natural or chemically synthesized small molecules
54 that bind to XPO1 and block the export of XPO1 cargo proteins from the nucleus to the cytoplasm
55 have been developed (9, 10). Collectively these molecules are known as selective inhibitors of
56 nuclear export (SINEs). SINEs have been shown to have anticancer activity against diverse types
57 of human cancers and at least one modified drug version with increased safety profile, called
58 Selinexor, has been approved by the FDA for treating multiple myeloma and diffuse large B-cell
59 lymphoma (11, 12). SINEs are also reported in the literature to have antiviral activity against RNA
60 viruses like influenza and respiratory syncytial virus (RSV) that causes respiratory infections due
61 to the blocking of key cellular processes and virus-mediated hijacking of the nucleocytoplasmic
62 transport process (6, 13, 14).

63 Coronaviruses are enveloped, positive-sense RNA viruses that are known to infect humans and
64 animals. At least seven coronaviruses are known to infect humans. Coronaviruses 229E, NL63,
65 OC43, and HKU1 infect people around the world to cause the common cold (15). Other
66 coronaviruses, MERS-CoV, SARS-CoV, and SARS-CoV-2, are responsible for major disease
67 outbreaks and cause high mortality (16). In nature, bats are known to be primary reservoirs of
68 many coronaviruses, from where viruses spill over to intermediate animals such as palm civet,

69 pangolins, rodents, camels, pigs, cattle where viruses evolve and then spillover to humans,
70 causing mild to severe disease (17, 18). The rapid emergence of different variants of SARS-CoV-
71 2 indicates that the viral genome acquire multiple mutations during replication (19, 20). In this
72 context, it is crucial to study the host factors and compounds that can enhance or reduce
73 replication of SARS-CoV-2 (21-25) .

74 We previously reported that XPO1 inhibitors, including leptomycin B (LMB) and Selinexor,
75 enhanced the replication of oncolytic myxoma virus (MYXV), a member of the leporipoxvirus
76 genus of *poxviridae,* in diverse types of cultured human cancer cells where intrinsic cellular
77 pathways restrict virus replication (26). Selinexor treatment reduced the formation of cytoplasmic
78 DHX9 antiviral granules, which are involved in lowering MYXV late protein synthesis and
79 replication (26). These findings led us to investigate further the role of Selinexor-mediated
80 inhibition of XPO1 nuclear export pathway on other viruses such as coronavirus.

81 Here, we show that Selinexor treatment can enhance coronavirus replication in a cell type specific
82 manner. Mouse Hepatitis Virus (MHV) replication was enhanced in both murine and human cell
83 lines. Furthermore, the targeted knockdown of XPO1 using siRNA also enhanced coronavirus
84 replication, suggesting the pro-coronavirus drug action is indeed related to the expected nuclear
85 export pathway target. However, SARS-CoV-2 replication remained unaffected in most of the cell
86 lines that were tested. These observations indicate that unlike other viruses, inhibition of nuclear
87 export pathway can have different effect on coronavirus replication in different cell types in vitro.

88 **Results**

89 **Nuclear export inhibitors enhance gene expression and replication of coronavirus in**
90 **murine L2 cells.**

91 Murine L2 cells are naturally infected by the mouse hepatitis virus (MHV). We first tested whether
92 inhibition of XPO1-mediated nuclear export pathway in L2 cells by different SINEs can alter the

93 replication of MHV. Since these compounds including Leptomycin B (LMB) are toxic to the cells
94 above 1μM concentration, we used lower concentrations that had minimal or no cytotoxicity to the
95 cells after 24 hours. To our surprise, all the tested SINEs, including LMB, significantly enhanced
96 MHV replication with a concentration of 0.1μM and 0.01μM (Fig 1 A-C). Compared to untreated
97 cells, treatment with XPO1 inhibitors Ratjadone enhanced virus titer almost 1.0 log, whereas
98 Anguinomycin and LMB enhanced virus titer about 0.7 log. Based on these results we next tested
99 the FDA approved anticancer nuclear export inhibitor Selinexor in our subsequent experiments.
100 We monitored and measured the viability of L2 cells in response to treatment with different
101 concentrations of Selinexor (Fig 2A). L2 cell viability was reduced only after treatment with a
102 Selinexor concentration of 5μM or above but had minimal or no effect with a concentration of 1
103 μM or less. To test the effect of Selinexor on MHV replication, L2 cells were first pretreated with
104 different concentrations of Selinexor for one hour and infected with a GFP-expressing MHV A59
105 (rA59/S_{MHV-2}-EGFP) to monitor the level of GFP expression in the infected cells (27-29). Infection
106 with this MHV exhibits reduced cell fusion since the virus expresses a less fusogenic form of the
107 spike protein and thus allowed counting the number of GFP positive cells. We observed increased
108 % of GFP expressing cells when pretreated with Selinexor. (Fig 2B). At 16 hpi, compared to
109 untreated cells, we observed significantly increased % of GFP positive cells after treatment with
110 more than 1μM selinexor. However, after 24 hpi, even 0.0001 μM selinexor treatment showed
111 significantly increased % of GFP expressing cells (Fig 2C). To assess the number of viruses
112 produced in the presence of Selinexor, L2 cells were treated with different concentration of
113 Selinexor and infected with another GFP expressing MHV A59 (MHVE-GFP) that expresses a
114 highly fusogenic form of spike and readily forms plaques. After 24h post infection, the infected
115 cells and supernatant were collected to titer the progeny virus formation by plaque assay. Virus
116 titration results show a significantly enhanced number of viruses in the cells pretreated with
117 Selinexor between 1 and 10 μM concentration (Fig 2D). These results confirm that Selinexor
118 enhances MHV replication and progeny virus formation in naturally permissive L2 cells.

119 **Selinexor enhances gene expression and replication of coronavirus in human cells.**

120 To further confirm the effects of Selinexor on MHV replication are not cell specific, we used human
121 cell lines expressing MHV receptor (MHVR) carcinoembryonic antigen-related cell adhesion
122 molecule 1 (CECAM1), HeLa-MHVR (human HeLa cell line expressing MHVR) (30) and A549-
123 CECAM/MHVR (human A549 cell line expressing MHVR) (31). Both cell lines were first treated
124 with different concentrations of Selinexor to test cell viability (Fig 3A and 4A). Unlike L2 cells,
125 Selinexor concentrations above 1μM significantly reduced viability of the human cells. However,
126 with a concentration of less than 0.1μM, we observed minimal or no reduction in cell viability. To
127 assess whether Selinexor enhances MHV replication in the human cell lines, both were pretreated
128 with different concentrations of Selinexor for one hour and infected with a GFP-expressing MHV,
129 rA59/S_{MHV-2}-EGFP to monitor GFP expression in the infected cells. We observed enhanced GFP
130 expressions when pretreated with Selinexor at a concentration of 0.01 μM or more (Fig 3B).
131 Enhanced GFP expression was further confirmed by counting the number of GFP-positive cells
132 (Fig 3C and 4B). To assess the amount of virus produced in the presence of Selinexor, HeLa-
133 MHVR (Fig 3D) and A549-MHVR (Fig 4C) cells were treated with different concentration of the
134 drug and infected with MHVE-GFP. Again, like L2 cells, we observed significantly enhanced virus
135 production in both the human cell lines when pretreated with Selinexor between 1 and 0.01 μM
136 concentration (Fig 3D and 4C).

137 **XPO1 knockdown enhances coronavirus gene expression and replication**

138 Since inhibition of the XPO1-mediated nuclear export pathway using Selinexor enhanced
139 coronavirus replication, we further extended this observation by direct knockdown of XPO1 using
140 siRNA. After transfection of XPO1 siRNA or a non-targeting control siRNA (NT-siRNA) in A549-
141 MHVR cells, the cells were infected with different MOIs of the GFP expressing MHV, rA59/S_{MHV-}
142 $_{2}$-EGFP or MHVE-GFP. An increase in GFP-expressing cells was observed only in the XPO1
143 knockdown cells (Fig 5A). Furthermore, the enhanced number of GFP-positive cells in the XPO1
144 knockdown cells compared to controls was confirmed by counting the number of GFP-positive

145 cells (Fig 5C). The level of XPO1 protein knockdown using siRNA was confirmed by western blot
146 analysis (Fig 5B). To quantify the number of progeny virions in the infected cells and supernatant,
147 the cells were infected with MHVE-GFP and samples were collected 24h post-infection. Virus
148 titration shows that virus production significantly increased in the XPO1 knockdown cells
149 compared to the NT-siRNA control or cells infected with the virus alone (Fig 5D), indicating that
150 the effect of Selinexor is mediated by XPO1.

151 **Effect of Selinexor on SARS-CoV-2 replication.**

152 We next tested whether Selinexor enhances the replication of SARS-CoV-2 in human cells. We
153 used a human A549 cell line expressing the ACE2 receptor ($A549^{ACE2}$) and a SARS-CoV-2 virus
154 expressing GFP (SARS-CoV-2-GFP) (32). The $A549^{ACE2}$ cell line showed a similar level of
155 sensitivity to different concentrations of Selinexor like A549-MHVR (data not shown). To assess
156 whether Selinexor enhances SARS-CoV-2 gene expression and replication, $A549^{ACE2}$ cells were
157 first pretreated with 0.01μM of Selinexor for one hour and infected with SARS-CoV-2-GFP. After
158 24h, cells were collected and fixed for counting the number of GFP-positive cells. A significantly
159 increased number of GFP-positive cells were observed in the treated infected cells compared to
160 the untreated cells (Fig 6A). We also observed a modest but significant increase in virus titer in
161 $A549^{ACE2}$cells (Fig 6B). The effect of Selinexor on SARS-CoV-2 was further tested using an
162 infectious recombinant SARS-CoV-2 (rSARS-CoV-2) virus (33-35). Like the parental SARS-CoV-
163 2 this recombinant virus titer was also increased in human A549 cells in the presence of Selinexor
164 (Fig 7A). However, in Vero and human Calu3 cells no significant increase or decrease in virus
165 titer was observed when treated with Selinexor (Fig 7B and 7C). These results indicate that,
166 unlike MHV, the effect of Selinexor on the replication of SARS-CoV-2 is cell type dependent.

167 **Discussion**

168 The nucleocytoplasmic transport process mediated by XPO1 plays a vital role in the export of
169 hundreds of proteins from the nucleus. The proteins are involved in diverse cellular processes

170 such as cell proliferation, cell cycle progression, and apoptosis (1, 5). Thus, the XPO1-mediated
171 export pathway is targeted by viruses at various stages of their lifecycle to regulate cellular
172 proteins and the appropriate localization of viral proteins (6, 36). Apart from viruses, this nuclear
173 export pathway is also crucial for anticancer therapy due to the export of tumor suppressor
174 proteins by XPO1 to the cytoplasm (7, 10). Therefore, XPO1 inhibitors are developed as potential
175 antiviral and anticancer agents. The cysteine residue within the hydrophobic nuclear export
176 sequence (NES)-binding region at position 528 is the prime target for most XPO1 inhibitors,
177 including leptomycin B (LMB). LMB isolated from Streptomyces was the first specific inhibitor of
178 XPO1 (37). However, the clinical development was discontinued due to severe cell toxicity (38).
179 The irreversible binding of LMB with CRM1 caused long-term inhibition of CRM1-mediated
180 nuclear export, and possible other off-target activity resulting in cellular toxicity (38). Synthetic
181 derivatives of LMB with less toxicity due to the reversible binding with CRM1 have been clinically
182 tested in human. The FDA has approved one such XPO1/CRM1 inhibitor called Selinexor for
183 treating hematological cancers (11). XPO1 inhibitors have shown antiviral activity against many
184 viruses, such as influenza, RSV, and recently SARS-CoV-2 (13, 25, 36, 39, 40).

185 We reported that, unlike RNA viruses, LMB or Selinexor enhances the replication of oncolytic
186 MYXV, a leporipoxvirus developed for cancer treatment (26). In human cancer cells, Selinexor
187 enhanced MYXV replication only at a low concentration that had minimal or no toxicity to the cells.
188 However, a higher concentration of Selinexor that caused cellular toxicity also reduced virus
189 replication. Based on our observation that nuclear export inhibitors, including Selinexor, can
190 enhance cytoplasmic replication of a poxvirus and a study showing that Selinexor inhibits SARS-
191 CoV-2 replication, we first tested the effect of different nuclear export inhibitors, including
192 Selinexor, on the replication of a mouse coronavirus MHV using murine L2 cells. To our surprise,
193 we observed that pretreatment of L2 cells with different concentrations of these inhibitors that had
194 minimal or no toxicity to the cells significantly increased the replication of MHV. This observation

195 was further confirmed using human HeLa and A549 cells expressing the MHV receptor murine
196 CECAM1(30). Again, increased reporter GFP expression and MHV replication were observed
197 when cells were pretreated with Selinexor concentrations that had minimal or no effect on the cell
198 viability. These results confirm that the impact of Selinexor on MHV replication is independent of
199 the cell type. Since XPO1 is the only known cellular target of Selinexor, we previously reported
200 that XPO1 knockdown using siRNA enhanced the replication of MYXV in human cancer cells (26).
201 Here, again, we confirmed that XPO1/CRM1 knockdown also significantly enhanced the
202 replication of MHV in both A549-MHVR and HeLa-MHVR cell lines. Both poxviruses and
203 coronaviruses replicate in the cytoplasm of infected cells. The observations that inhibition of
204 XPO1-mediated nuclear export pathway can enhance the replication of both the viruses suggest
205 the importance of this pathway for future studies to identify the host and viral proteins involved in
206 this process. These results encouraged us to test whether the optimized lower concentration of
207 Selinexor enhances SARS-CoV-2 replication in different cell types. However, unlike MHV,
208 Selinexor-mediated enhanced SARS-CoV-2 replication was observed only in selected cell lines
209 and had no significant effect on virus replication in other cell lines, such as Vero-E6 and Calu3.
210 This observation is in contrast to a previous study by Kashyap et al. showing that in Vero E6
211 cells, Selinexor treatment reduced the SARS-CoV-2 plaque number and virus titer by more than
212 two logs with >100nM Selinexor (25). In our study we did not observe any reduction in virus titer
213 with the tested concentration of Selinexor in any of the cell lines that we tested with both MHV
214 and SARS-CoV-2. The Selinexor concentration we used in our study had no or very minimal
215 toxicity to the cells. However, at higher concentration of Selinexor (>100nM), we observed
216 enhanced toxicity to the cells and can inhibit virus replication. We observed the cell type specific
217 effect of selinexor on myxoma virus, where selinexor did not affect virus replication in rabbit RK13
218 cells and Vero-E6 cells (data not shown). Therefore, we can speculate that different cell types
219 might respond to Selinexor differently against these tested viruses. Inhibition of XPO1-mediated
220 nuclear export pathway results in several changes in the cells, such as cell cycle arrest, and

221 modulation of cellular key signaling pathways regulating the expression of proinflammatory
222 cytokines. Depending on the cell type, these cellular changes might impact the virus replication
223 (41).

224 Selinexor is currently approved for treating selected hematological malignancies such as multiple
225 myeloma and diffuse large B-cell lymphoma (11, 42). Multiple clinical trials are presently
226 undergoing to use Selinexor as a monotherapy or in combination with other treatments against
227 diverse types of malignancies (43, 44). Our results indicate that Selinexor mediated inhibition of
228 nuclear export pathway might have different effect on virus replication. Future studies should
229 focus on how Selinexor and nuclear transportation pathway regulate the replication of
230 coronavirus.

231 **Materials and methods**

232 **Biosafety.**

233 SARS-CoV-2-GFP virus infections and virus manipulations were conducted at biosafety level 3
234 (BSL-3) and rSARS-CoV-2 Δ3a/Δ7b virus experiments were conducted at BSL-2+ level in the
235 Biodesign Institute at ASU using appropriate and IBC approved personal protective equipment
236 and protocols.

237 **Cell lines**

238 L2 murine fibroblast cell line and African green monkey kidney Vero cells E6 (obtained from
239 ATCC) were cultured and maintained using Dulbecco's modified Eagle's medium (DMEM)
240 supplemented with 10% FBS, 100 U/ml of penicillin, and 100 µg/ml streptomycin. Calu-3 cells
241 (ATCC: HTB-55) were cultured and maintained using Eagle's Minimum Essential Medium
242 (EMEM) supplemented with 10% FBS, 100 U/ml of penicillin, and 100 µg/ml streptomycin. HeLa-
243 MHVR cell line (human HeLa cell line expressing mouse coronavirus receptor mCECAM1) was
244 provided by Tom Gallagher at Loyola University and maintained using DMEM media with 10%

245 FBS, HEPES buffer, 100 U/ml of penicillin, 100 µg/ml streptomycin, MEM non-essential amino
246 acids, and sodium pyruvate. Human A549 cells expressing ACE2 and TMPRSS2 (ACE2plusC3-
247 A549/ACE2/TMPRSS2) was purchased from ATCC (CRL-3560) and maintained with DMEM
248 media supplemented with 10% FBS, 100 U/ml of penicillin, and 100 µg/ml streptomycin. A549-
249 MHVR (human A549 cell line expressing mouse coronavirus receptor mCECAM1) and $A549^{ACE2}$
250 (human A549 cell line expressing ACE2 receptor) was provided by Susan Weiss at the Perelman
251 School of Medicine at the University of Pennsylvania and maintained with RPMI1640 media
252 supplemented with 10% FBS, 100 U/ml of penicillin, and 100 µg/ml streptomycin (31).

253 **Viruses and viral replication assay**

254 Mouse hepatitis coronavirus MHV A59 that expresses GFP was used for all the assays.
255 rA59/S_{MHV-2}-EGFP is a recombinant MHV A59 virus that expresses the spike of MHV-2 in place
256 of the WT protein and GFP (27-29). MHVE-GFP was constructed using a MHV A59 reverse
257 genetics system essentially as previously described (45-48). The coding sequence for the MHV
258 envelope (E) protein was fused to the GFP gene with an intervening tetra glycine linker. The
259 construct was cloned into ORF 4a/b in the G subclone of the MHV infectious clone using SbfI and
260 EcoRV restriction sites. The construct was designed to maintain the transcription regulatory
261 sequences for both ORF 4 and ORF5. Virus was recovered after assembling the full-length
262 genomic cDNA and transcription of full-length genomic RNA as previously described (45-48).
263 Following electroporation into baby hamster kidney grown in 17Cl1 mouse cells virus was
264 recovered and passage 1 stock was grown in mouse 17Cl1 cells and titered in L2 cells by
265 plaque assay. The SARS-CoV-2-GFP virus was provided by Ralph Baric at the University of
266 North Carolina Chapel Hill (32).

267 Viral titers in different cell lines were determined using a viral replication assay. The cells were
268 seeded in 24 well plate ($2x10^5$ cells/well). The next day, the cells were treated for 1h with different
269 concentrations of nuclear export inhibitors diluted in the appropriate media used for growth of the

270 specific cell lines. Virus was added to the cells (volume calculated based on different multiplicities
271 of infection and incubated for 1h at 37°C in the presence of the inhibitors. After 1h, the unbound
272 virus was removed, cells were washed with DPBS (Dulbecco's phosphate-buffered saline) and
273 media with inhibitors was added for further incubation. Both cells and media were collected at
274 different time points and stored at -80°C freezer until processing. Afterwards, different dilutions
275 were prepared in the appropriate media and plated on cell lines and fluorescent foci were counted
276 after 24h using a fluorescent microscope. All assays and dilutions were performed in triplicate.
277 For SARS-CoV-2, all infections and virus manipulations were conducted at biosafety level 3 (BSL-
278 3) in the Biodesign Institute using appropriate and IBC-approved personal protective equipment
279 and protocols. For plaque assay, samples were serially diluted 10-fold and absorbed on Vero
280 cells at 37°C for 1h. Cells were overlaid with media plus 0.7% agarose and incubated for two days
281 at 37°C. Cells were fixed with 4% paraformaldehyde and subsequently stained with 1% crystal
282 violet for counting the plaques.

283 **Reagents and Antibodies**

284 Rabbit polyclonal antibodies for XPO1, ACE-2 and mouse monoclonal antibody against β-actin
285 were purchased from Thermo Fisher Scientific. HRP-conjugated goat anti-rabbit and anti-
286 mouse IgG antibodies were purchased from Jackson Immuno Research Laboratories.
287 Selinexor (KPT330) was purchased from Apex Bio (Tokyo, Japan). Leptomycin B, Ratjadone
288 A, and Anguinomycin A purchased from Santa Cruz Biotechnology.

289 **siRNA transfection**

290 ON-TARGETplus SMART pool siRNAs for exportin 1/XPO1 and a non-targeting control (NT
291 siRNA) were purchased from Dharmacon (Horizon Discovery). In 24 well plate cells were
292 seeded with 40–50% confluence, left overnight for adherence, and then transfected with
293 siRNAs (40 nM) using Lipofectamine RNAiMAX (Invitrogen) transfection reagent. After 48 h of

294 transfection, the cells were infected with different MOIs of virus for 1h, washed to remove the
295 unbound virus, and incubated with complete media. At the indicated time points, cells were
296 either observed by fluorescence microscopy to monitor and record the expression of
297 fluorescent proteins or harvested and processed for titration of progeny virions. For detection
298 of proteins, Western blot analysis was performed from the total proteins as described before
299 (49).

300 **Cell viability assay**

301 To assess the viability of different cell lines after Selinexor treatment, 10,000 cells were seeded
302 into each well of a 96-well plate. The next day, cells were treated with different concentrations of
303 Selinexor. A minimum of four to five wells were used for each treatment condition, and untreated
304 cells (mock) served as controls. Cell viability at different time points was assessed using MTS
305 reagents (Promega) according to manufacturer instructions.

306 **Statistical analysis**

307 Statistical analyses were performed using GraphPad Prism software. Values are represented as
308 mean ± SD for at least two or three independent experiments. ANOVA and t-test (when only two
309 groups were compared) were used to determine the significance. *P* values are reported as
310 follows: no significant (ns) $P > 0.05$, * $P < 0.05$, ** $P < 0.01$, *** $P < 0.001$, **** $P < 0.0001$.

311 **Acknowledgements**

312 We thank Tom Gallagher (Loyola University) for the HeLa-MHVR cells; Susan Weiss (Perelman
313 School of Medicine at the University of Pennsylvania) for the A549-MHVR cells, $A549^{ACE2}$ cells
314 and rA59/S_{MHV-2}-EGFP virus; Ralph Baric (University of North Carolina at Chapel Hill) for the
315 SARS-CoV-2-GFP virus; Luis Martinez-Sobrido at the Texas Biomedical Research Institute,
316 San Antonio, TX for rSARS-CoV-2 Δ3a/Δ7b virus; and Efrem Lim and Emily Kaelin (Biodesign
317 Institute, Arizona State University) for performing SARS-CoV-2 qRT-PCR assay.

318 **Funding Statement**

319 This research was supported by grants from the National Institute of Health (NIH) USA R01
320 AI080607 and R21 AI163910 to M.M.R.; an Arizona Biomedical Research Center (ABRC)
321 Investigator Award RFGA2022-010-22 to M.M.R.; an Arizona State University (Tempe, Arizona,
322 USA) start-up grant to M.M.R.; a Mercatus Center Fast Grant (G09202-300) to G.M., M.M.R, and
323 B.G.H.; NIH R01DK048370-26 Subaward VUMC95054 to B.G.H.; and Tohono O'Odham Nation
324 Award GR40818 to B.G.H.

325 The funders had no role in the study design, data collection and interpretation, or decision to
326 submit the work for publication.

327 **References:**

328 1. Wing CE, Fung HYJ, Chook YM. 2022. Karyopherin-mediated nucleocytoplasmic transport. Nat Rev
329 Mol Cell Biol 23:307-328.
330 2. Tetenbaum-Novatt J, Rout MP. 2010. The mechanism of nucleocytoplasmic transport through the
331 nuclear pore complex. Cold Spring Harb Symp Quant Biol 75:567-84.
332 3. Kumar AV, Kang T, Thakurta TG, Ng C, Rogers AN, Larsen MR, Lapierre LR. 2022. Exportin 1
333 modulates life span by regulating nucleolar dynamics via the autophagy protein LGG-1/GABARAP.
334 Sci Adv 8:eabj1604.
335 4. Ishikawa C, Mori N. 2022. Exportin-1 is critical for cell proliferation and survival in adult T cell
336 leukemia. Invest New Drugs 40:718-727.
337 5. Azmi AS, Uddin MH, Mohammad RM. 2021. The nuclear export protein XPO1 - from biology to
338 targeted therapy. Nat Rev Clin Oncol 18:152-169.
339 6. Uddin MH, Zonder JA, Azmi AS. 2020. Exportin 1 inhibition as antiviral therapy. Drug Discov Today
340 25:1775-1781.
341 7. Azizian NG, Li Y. 2020. XPO1-dependent nuclear export as a target for cancer therapy. J Hematol
342 Oncol 13:61.
343 8. Zhao L, Luo B, Wang L, Chen W, Jiang M, Zhang N. 2021. Pan-cancer analysis reveals the roles of
344 XPO1 in predicting prognosis and tumorigenesis. Transl Cancer Res 10:4664-4679.
345 9. Jans DA, Martin AJ, Wagstaff KM. 2019. Inhibitors of nuclear transport. Curr Opin Cell Biol 58:50-
346 60.
347 10. Gerecitano J. 2014. SINE (selective inhibitor of nuclear export)--translational science in a new class
348 of anti-cancer agents. J Hematol Oncol 7:67.
349 11. Goldsmith SR, Liu L, Shiah K. 2022. Selinexor therapy for multiple myeloma and non-Hodgkin
350 lymphomas. Curr Opin Oncol 34:524-530.
351 12. Lassman AB, Wen PY, van den Bent MJ, Plotkin SR, Walenkamp AME, Green AL, Li K, Walker CJ,
352 Chang H, Tamir S, Henegar L, Shen Y, Alvarez MJ, Califano A, Landesman Y, Kauffman MG,
353 Shacham S, Mau-Sørensen M. 2022. A Phase II Study of the Efficacy and Safety of Oral Selinexor
354 in Recurrent Glioblastoma. Clin Cancer Res 28:452-460.

355 13. Pickens JA, Tripp RA. 2018. Verdinexor Targeting of CRM1 is a Promising Therapeutic Approach
356 against RSV and Influenza Viruses. Viruses 10.
357 14. Sajidah ES, Lim K, Wong RW. 2021. How SARS-CoV-2 and Other Viruses Build an Invasion Route to
358 Hijack the Host Nucleocytoplasmic Trafficking System. Cells 10.
359 15. Paules CI, Marston HD, Fauci AS. 2020. Coronavirus Infections-More Than Just the Common Cold.
360 Jama 323:707-708.
361 16. V'Kovski P, Kratzel A, Steiner S, Stalder H, Thiel V. 2021. Coronavirus biology and replication:
362 implications for SARS-CoV-2. Nat Rev Microbiol 19:155-170.
363 17. Fung TS, Liu DX. 2019. Human Coronavirus: Host-Pathogen Interaction. Annu Rev Microbiol
364 73:529-557.
365 18. Zhang T, Wu Q, Zhang Z. 2020. Probable Pangolin Origin of SARS-CoV-2 Associated with the COVID-
366 19 Outbreak. Curr Biol 30:1346-1351.e2.
367 19. Mahilkar S, Agrawal S, Chaudhary S, Parikh S, Sonkar SC, Verma DK, Chitalia V, Mehta D, Koner BC,
368 Vijay N, Shastri J, Sunil S. 2022. SARS-CoV-2 variants: Impact on biological and clinical outcome.
369 Front Med (Lausanne) 9:995960.
370 20. Wiegand T, Nemudryi A, Nemudraia A, McVey A, Little A, Taylor DN, Walk ST, Wiedenheft B. 2022.
371 The Rise and Fall of SARS-CoV-2 Variants and Ongoing Diversification of Omicron. Viruses 14.
372 21. Madden EA, Diamond MS. 2022. Host cell-intrinsic innate immune recognition of SARS-CoV-2.
373 Curr Opin Virol 52:30-38.
374 22. Lv L, Zhang L. 2021. Host proviral and antiviral factors for SARS-CoV-2. Virus Genes 57:475-488.
375 23. Baggen J, Vanstreels E, Jansen S, Daelemans D. 2021. Cellular host factors for SARS-CoV-2
376 infection. Nat Microbiol 6:1219-1232.
377 24. Narayanan A, Narwal M, Majowicz SA, Varricchio C, Toner SA, Ballatore C, Brancale A, Murakami
378 KS, Jose J. 2022. Identification of SARS-CoV-2 inhibitors targeting Mpro and PLpro using in-cell-
379 protease assay. Commun Biol 5:169.
380 25. Kashyap T, Murray J, Walker CJ, Chang H, Tamir S, Hou B, Shacham S, Kauffman MG, Tripp RA,
381 Landesman Y. 2021. Selinexor, a novel selective inhibitor of nuclear export, reduces SARS-CoV-2
382 infection and protects the respiratory system in vivo. Antiviral Res 192:105115.
383 26. Rahman MM, van Oosterom F, Enow JA, Hossain M, Gutierrez-Jensen AD, Cashen M, Everts A,
384 Lowe K, Kilbourne J, Daggett-Vondras J, Karr TL, McFadden G. 2023. Nuclear Export Inhibitor
385 Selinexor Enhances Oncolytic Myxoma Virus Therapy against Cancer. Cancer Res Commun 3:952-
386 968.
387 27. Das Sarma J, Fu L, Tsai JC, Weiss SR, Lavi E. 2000. Demyelination determinants map to the spike
388 glycoprotein gene of coronavirus mouse hepatitis virus. J Virol 74:9206-13.
389 28. Das Sarma J, Iacono K, Gard L, Marek R, Kenyon LC, Koval M, Weiss SR. 2008. Demyelinating and
390 nondemyelinating strains of mouse hepatitis virus differ in their neural cell tropism. J Virol
391 82:5519-26.
392 29. Qiu Z, Hingley ST, Simmons G, Yu C, Das Sarma J, Bates P, Weiss SR. 2006. Endosomal proteolysis
393 by cathepsins is necessary for murine coronavirus mouse hepatitis virus type 2 spike-mediated
394 entry. J Virol 80:5768-76.
395 30. Rao PV, Gallagher TM. 1998. Intracellular complexes of viral spike and cellular receptor
396 accumulate during cytopathic murine coronavirus infections. J Virol 72:3278-88.
397 31. Li Y, Renner DM, Comar CE, Whelan JN, Reyes HM, Cardenas-Diaz FL, Truitt R, Tan LH, Dong B,
398 Alysandratos KD, Huang J, Palmer JN, Adappa ND, Kohanski MA, Kotton DN, Silverman RH, Yang
399 W, Morrisey EE, Cohen NA, Weiss SR. 2021. SARS-CoV-2 induces double-stranded RNA-mediated
400 innate immune responses in respiratory epithelial-derived cells and cardiomyocytes. Proc Natl
401 Acad Sci U S A 118.

402 32. Hou YJ, Okuda K, Edwards CE, Martinez DR, Asakura T, Dinnon KH, 3rd, Kato T, Lee RE, Yount BL,
403 Mascenik TM, Chen G, Olivier KN, Ghio A, Tse LV, Leist SR, Gralinski LE, Schäfer A, Dang H, Gilmore
404 R, Nakano S, Sun L, Fulcher ML, Livraghi-Butrico A, Nicely NI, Cameron M, Cameron C, Kelvin DJ,
405 de Silva A, Margolis DM, Markmann A, Bartelt L, Zumwalt R, Martinez FJ, Salvatore SP, Borczuk A,
406 Tata PR, Sontake V, Kimple A, Jaspers I, O'Neal WK, Randell SH, Boucher RC, Baric RS. 2020. SARS-
407 CoV-2 Reverse Genetics Reveals a Variable Infection Gradient in the Respiratory Tract. Cell
408 182:429-446.e14.
409 33. Ye C, Chiem K, Park JG, Oladunni F, Platt RN, 2nd, Anderson T, Almazan F, de la Torre JC, Martinez-
410 Sobrido L. 2020. Rescue of SARS-CoV-2 from a Single Bacterial Artificial Chromosome. mBio 11.
411 34. Ye C, Park JG, Chiem K, Dravid P, Allué-Guardia A, Garcia-Vilanova A, Pino Tamayo P, Shivanna V,
412 Kapoor A, Walter MR, Kobie JJ, Plemper RK, Torrelles JB, Martinez-Sobrido L. 2023. Immunization
413 with Recombinant Accessory Protein-Deficient SARS-CoV-2 Protects against Lethal Challenge and
414 Viral Transmission. Microbiol Spectr 11:e0065323.
415 35. Silvas JA, Vasquez DM, Park JG, Chiem K, Allué-Guardia A, Garcia-Vilanova A, Platt RN, Miorin L,
416 Kehrer T, Cupic A, Gonzalez-Reiche AS, Bakel HV, García-Sastre A, Anderson T, Torrelles JB, Ye C,
417 Martinez-Sobrido L. 2021. Contribution of SARS-CoV-2 Accessory Proteins to Viral Pathogenicity
418 in K18 Human ACE2 Transgenic Mice. J Virol 95:e0040221.
419 36. Mathew C, Ghildyal R. 2017. CRM1 Inhibitors for Antiviral Therapy. Front Microbiol 8:1171.
420 37. Ferreira BI, Cautain B, Grenho I, Link W. 2020. Small Molecule Inhibitors of CRM1. Front Pharmacol
421 11:625.
422 38. Newlands ES, Rustin GJ, Brampton MH. 1996. Phase I trial of elactocin. Br J Cancer 74:648-9.
423 39. Perwitasari O, Johnson S, Yan X, Howerth E, Shacham S, Landesman Y, Baloglu E, McCauley D,
424 Tamir S, Tompkins SM, Tripp RA. 2014. Verdinexor, a novel selective inhibitor of nuclear export,
425 reduces influenza a virus replication in vitro and in vivo. J Virol 88:10228-43.
426 40. Mathew C, Tamir S, Tripp RA, Ghildyal R. 2021. Reversible disruption of XPO1-mediated nuclear
427 export inhibits respiratory syncytial virus (RSV) replication. Sci Rep 11:19223.
428 41. Li D, Fang H, Zhang R, Xie Q, Yang Y, Chen L. 2024. Beyond oncology: Selinexor's journey into anti-
429 inflammatory treatment and long-term management. Front Immunol 15:1398927.
430 42. Nachmias B, Schimmer AD. 2020. Targeting nuclear import and export in hematological
431 malignancies. Leukemia 34:2875-2886.
432 43. Landes JR, Moore SA, Bartley BR, Doan HQ, Rady PL, Tyring SK. 2022. The efficacy of selinexor
433 (KPT-330), an XPO1 inhibitor, on non-hematologic cancers: a comprehensive review. J Cancer Res
434 Clin Oncol doi:10.1007/s00432-022-04247-z.
435 44. Galinski B, Alexander TB, Mitchell DA, Chatwin HV, Awah C, Green AL, Weiser DA. 2021.
436 Therapeutic Targeting of Exportin-1 in Childhood Cancer. Cancers (Basel) 13.
437 45. Verma S, Lopez LA, Bednar V, Hogue BG. 2007. Importance of the penultimate positive charge in
438 mouse hepatitis coronavirus A59 membrane protein. JVirol 81:5339-5348.
439 46. Ye Y, Hogue BG. 2007. Role of the coronavirus E viroporin protein transmembrane domain in virus
440 assembly. JVirol 81:3597-3607.
441 47. Lopez LA, Riffle AJ, Pike SL, Gardner D, Hogue BG. 2008. Importance of conserved cysteine
442 residues in the coronavirus envelope protein. JVirol 82:3000-3010.
443 48. Arndt AL, Larson BJ, Hogue BG. 2010. A conserved domain in the coronavirus membrane protein
444 tail is important for virus assembly. JVirol 84:11418-11428.
445 49. Rahman MM, Bagdassarian E, Ali MAM, McFadden G. 2017. Identification of host DEAD-box RNA
446 helicases that regulate cellular tropism of oncolytic Myxoma virus in human cancer cells. Sci Rep
447 7:15710.

448

449 **Figure Legends**

450 Figure 1: Nuclear export inhibitors enhance the replication of MHV in L2 cells. L2 cells were plated
451 in 24 well plates, treated with the indicated concentration of nuclear export inhibitors: A)
452 Ratjadone, B) Anguinomycin, and C) Leptomycin B for 1h and infected with MHVE-GFP virus with
453 a MOI of 0.01. Virus replication was measured by plaque assay from the total number of viruses
454 in the cells and supernatant 24h post infection. Data represents ± SD and n=3. Statistically
455 significant differences in comparison to 24 hpi infection are indicated. ^{ns} $P > 0.05$, * $P < 0.05$, ** P
456 < 0.01, *** $P < 0.001$, **** $P < 0.0001$.

457 Figure 2: Selinexor enhances the replication of MHV in L2 cells. A) Effect of Selinexor on L2 cells
458 viability. Cells were plated in 96 well plates and treated with different concentration of Selinexor
459 and cell viability was measured after 48h. B-D) Effect of Selinexor on MHV virus gene expression
460 and replication. Cells were plated in 24 well plates, treated with the indicated concentration of
461 Selinexor for 1h and infected with rA59/S_{MHV-2}-EGFP or MHVE-GFP virus with a MOI of 0.01. B)
462 Fluorescence images were taken 24h post infection with rA59/S_{MHV-2}-EGFP; C) percent of GFP
463 positive cells were counted using Countess II cell counter at different time points after infection
464 with rA59/S_{MHV-2}-EGFP; D) MHVE-GFP virus replication was measured by plaque assay from the
465 total number of viruses in the cells and supernatant 24h post infection. Data represents ± SD and
466 n=3. Statistically significant differences in comparison to control are indicated. ^{ns} $P > 0.05$, * $P <$
467 0.05, ** $P < 0.01$, *** $P < 0.001$.

468 Figure 3: Selinexor enhances the replication of MHV in human HeLa-MHVR cells. A) Effect of
469 Selinexor on the viability of HeLa-MHVR cells. Cells were plated in 96 well plates and treated with
470 different concentration of Selinexor and cell viability was measured after 48h. B-D) Effect of
471 Selinexor on MHV virus replication in HeLa-MHVR cells. Cells were plated in 24 well plates,
472 treated with indicated concentration of Selinexor for 1h and infected with rA59/S_{MHV-2}-EGFP or
473 MHVE-GFP virus with a MOI of 0.01. B) Fluorescence images were taken 24h post infection with

474 rA59/S_{MHV-2}-EGFP; C) percent of GFP positive cells at 24h and 48h post infection with rA59/S_{MHV-}
475 $_{2}$-EGFP were counted using Countess II cell counter; D) Total number of viruses in the cells and
476 supernatant was determined by plaque assay 24h post infection of cells with MHVE-GFP. Data
477 represents ± SD and n=3. Statistically significant differences in comparison to control are
478 indicated. ^{ns} $P > 0.05$, * $P < 0.05$, ** $P < 0.01$, *** $P < 0.001$, **** $P < 0.0001$.

479 Figure 4: Selinexor enhances the replication of MHV in human A549-MHVR cells. A) Effect of
480 Selinexor on the viability of A549-MHVR cells. Cells were plated in 96 well plates and treated with
481 different concentration of Selinexor and cell viability was measured after 48h. B-C) Effect of
482 Selinexor on MHV virus replication in A549-MHVR cells. Cells were plated in 24 well plates,
483 treated with indicated concentration of Selinexor for 1h and infected with rA59/S_{MHV-2}-EGFP or
484 MHVE-GFP virus with a MOI of 0.01. B) percent of GFP positive cells at 24h and 48h post infection
485 with rA59/S_{MHV-2}-EGFP were counted using Countess II cell counter; C) Total number of viruses
486 in the cells and supernatant was determined by plaque assay 24h post infection of cells with
487 MHVE-GFP. Data represents ± SD and n=3. Statistically significant differences in comparison to
488 control are indicated. ^{ns} $P > 0.05$, * $P < 0.05$, ** $P < 0.01$, *** $P < 0.001$.

489 Figure 5: XPO1 knock down enhances the replication of MHV in human A549-CECAM cells. Cells
490 were plated in 24 well plates, transfected with control non-targeting siRNA (NT-siRNA) or XPO1
491 siRNA for 48h and infected with rA59/S_{MHV-2}-EGFP or MHVE-GFP for another 24h. A) Images
492 were taken using a fluorescence microscope 24h post infection with MHVE-GFP; B) Knock down
493 of XPO1 was confirmed with Western blot analysis using anti-XPO1 antibody. Actin was used as
494 total protein loading control. C) percent of GFP positive cells after infection with rA59/S_{MHV-2}-EGFP
495 were counted using Countess II cell counter. D) Total number of viruses in the cells and
496 supernatant was determined by plaque assay 24h post infection of cells with MHVE-GFP. Data
497 represents ± SD and n=3 or 4. Statistically significant differences in comparison to control are
498 indicated. ^{ns} $P > 0.05$, * $P < 0.05$, ** $P < 0.01$, *** $P < 0.001$.

499 Figure 6: Selinexor enhances the replication of SARS-CoV-2 in human A549^{ACE2} cells. Cells were
500 plated in 12 well plates, treated with indicated concentration of Selinexor for 1h and infected with
501 SARS-CoV-2 virus. A) percent of GFP positive cells were counted using Countess II cell counter
502 after fixation of cells. B) Total number of progeny virus formation was measured by plaque assay
503 using Vero E6 cells. Data represents ± SD and n=3 or 4. Statistically significant differences in
504 comparison to control are indicated. ^{ns} $P > 0.05$, * $P < 0.05$, ** $P < 0.01$, *** $P < 0.001$.

505 Figure 7: Effect of Selinexor on the replication of rSARS-CoV-2 in different cell types. A) Human
506 A549^{A2T2} cells, B) Vero E6 cells, and C) Human Calu3 cells were plated in 12 well plates, treated
507 with indicated concentration of Selinexor for 1h and infected with rSARS-CoV-2 virus with a MOI
508 of 0.1. Total number of progeny virus formation was measured by plaque assay using Vero E6
509 cells. Data represents ± SD and n=3 or 4. Statistically significant differences in comparison to
510 control are indicated. ^{ns} $P > 0.05$, * $P < 0.05$.

511

512

513

514

515

Figure 1

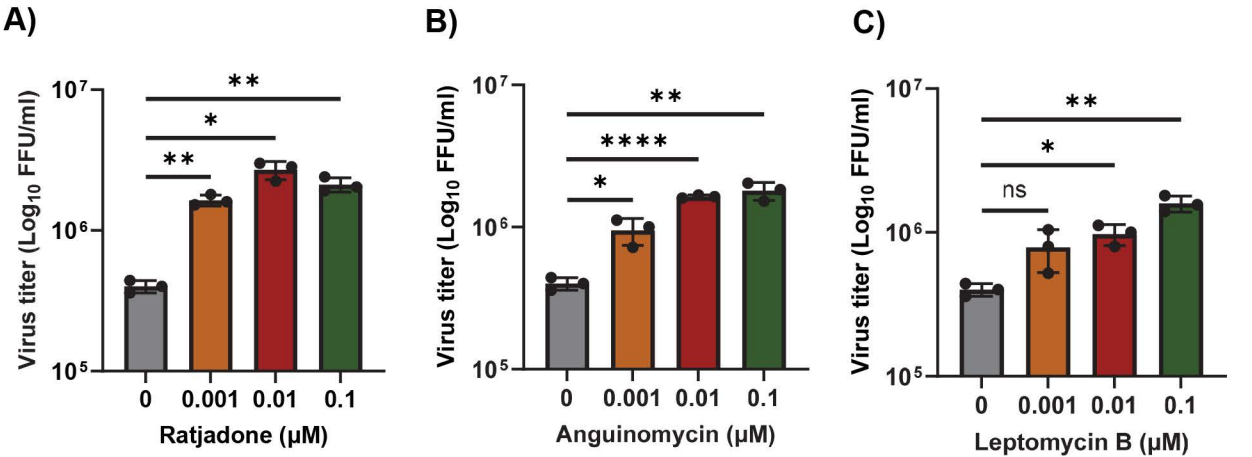
A)
B)
C)
Virus titer (Log10 FFU/ml)
10^7
10^6
10^5
**
*
****
ns
0
0.001
0.01
0.1
Ratjadone (μM)
Anguinomycin (μM)
Leptomycin B (μM)

Figure 2

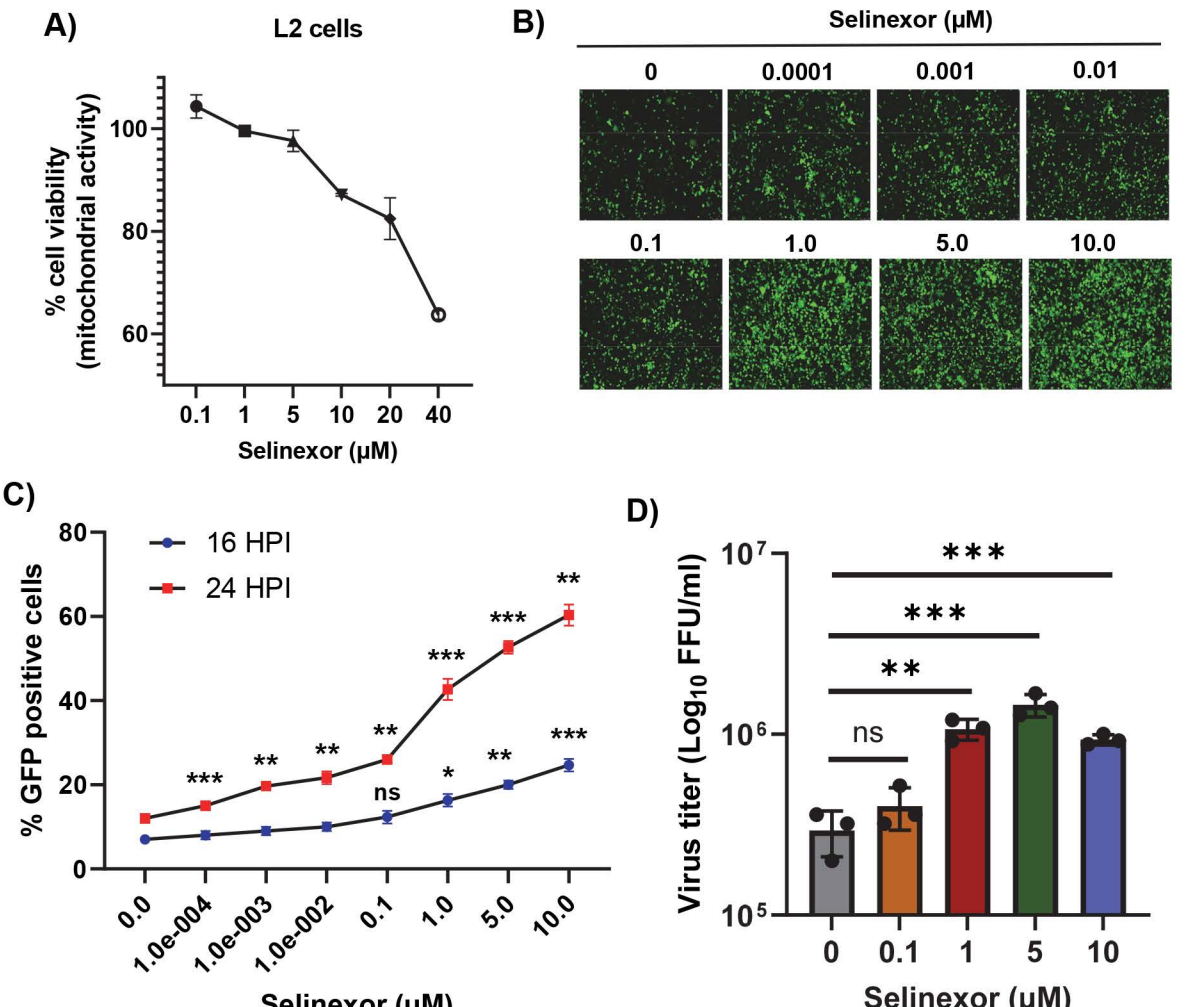
A)
L2 cells
% cell viability
(mitochondrial activity)
100
80
60
0.1
1
5
10
20
40
Selinexor (μM)
B)
Selinexor (μM)
0
0.0001
0.001
0.01
0.1
1.0
5.0
10.0
C)
16 HPI
24 HPI
% GFP positive cells
80
60
40
20
0
***
**
**
**
ns
***
***
*
**
**
***
0.0
1.0e-004
1.0e-003
1.0e-002
0.1
1.0
5.0
10.0
Selinexor (μM)
D)
Virus titer (Log10 FFU/ml)
10^7
10^6
10^5
***
***
**
ns
0
0.1
1
5
10
Selinexor (μM)

Figure 3

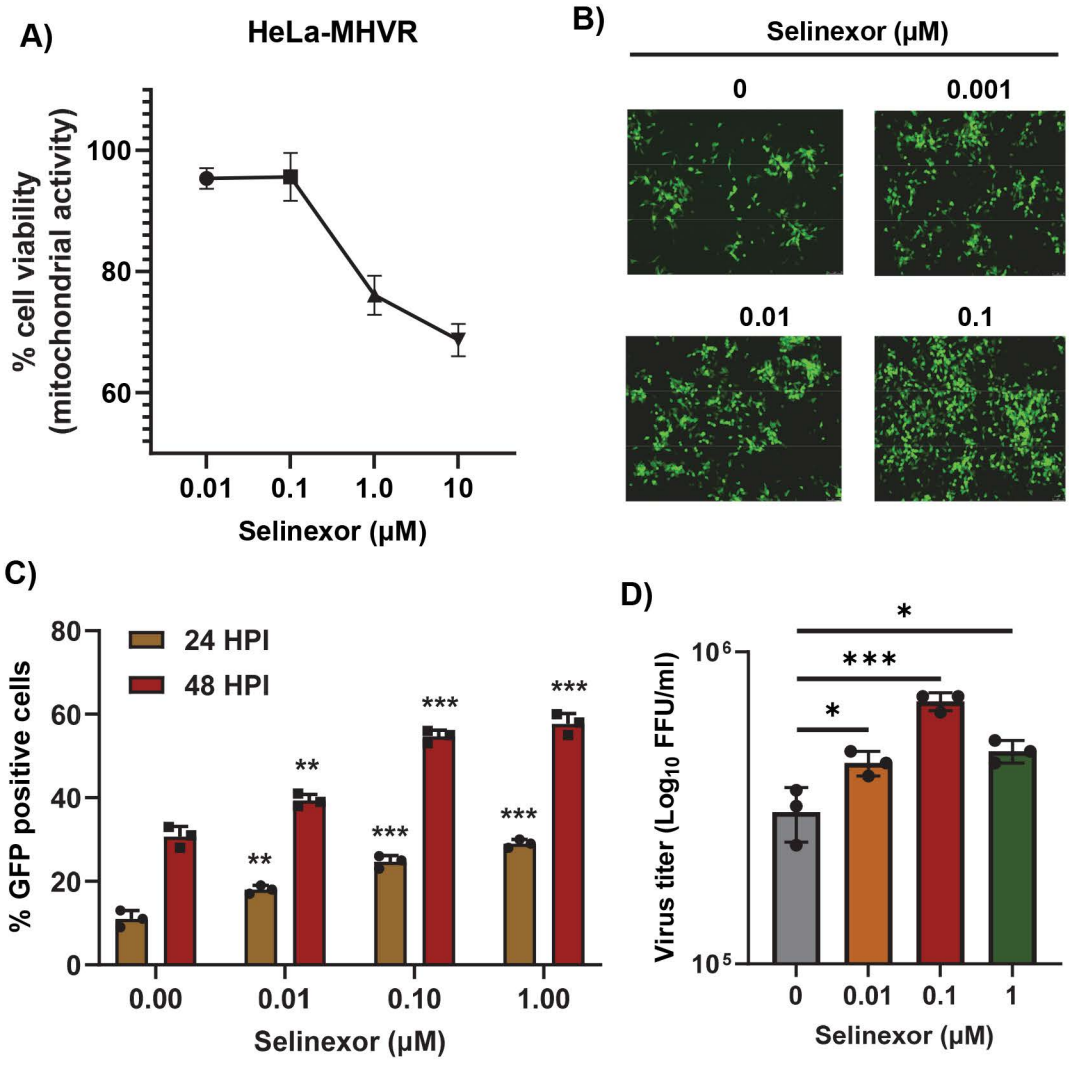
A)
HeLa-MHVR
% cell viability
(mitochondrial activity)
100
80
60
0.01
0.1
1.0
10
Selinexor (μM)
B)
Selinexor (μM)
0
0.001
0.01
0.1
C)
24 HPI
48 HPI
% GFP positive cells
80
60
40
20
0
**
**
***
***
***
***
0.00
0.01
0.10
1.00
Selinexor (μM)
D)
*
***
*
Virus titer (Log10 FFU/ml)
10^6
10^5
0
0.01
0.1
1
Selinexor (μM)

Figure 4

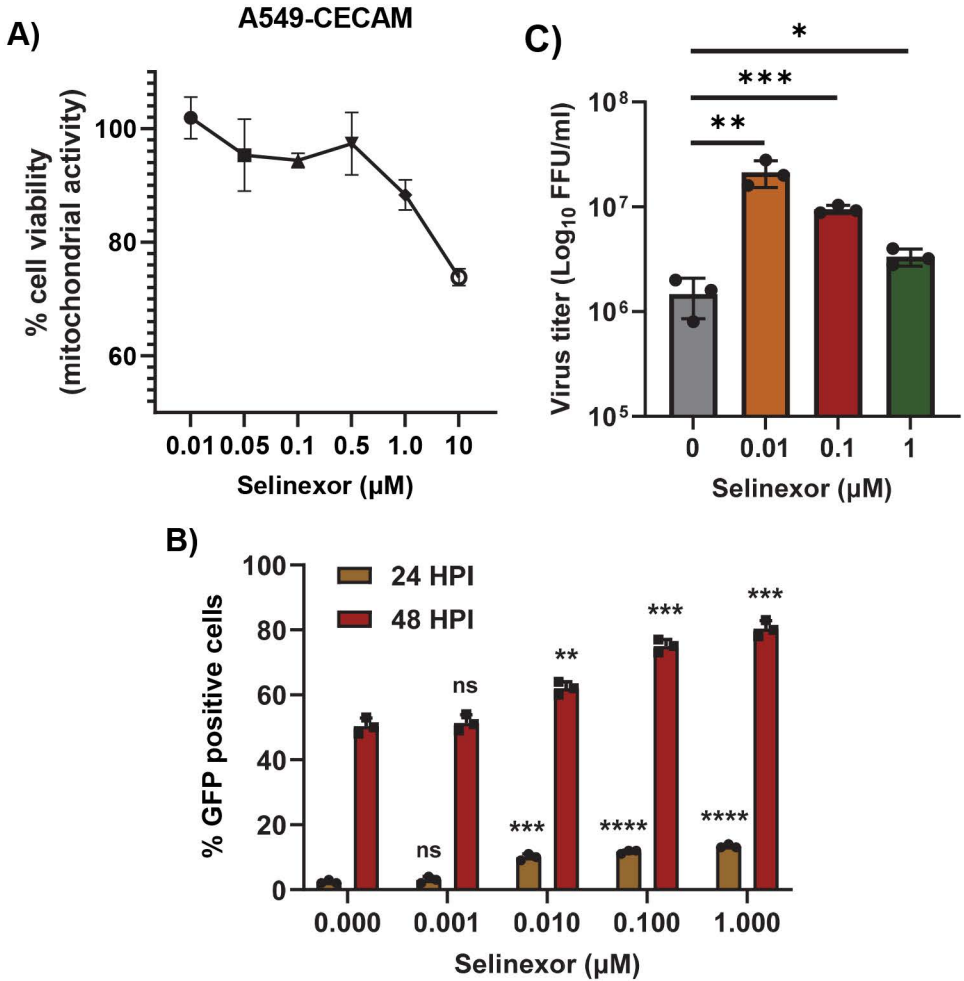
A)
A549-CECAM
% cell viability
(mitochondrial activity)
100
80
60
0.01 0.05 0.1 0.5 1.0 10
Selinexor (μM)
C)
*
***
**
Virus titer (Log10 FFU/ml)
10^8
10^7
10^6
10^5
0 0.01 0.1 1
Selinexor (μM)
B)
24 HPI
48 HPI
% GFP positive cells
100
80
60
40
20
0
ns
ns
**
***
***
****
***
****
0.000 0.001 0.010 0.100 1.000
Selinexor (μM)

Figure 5

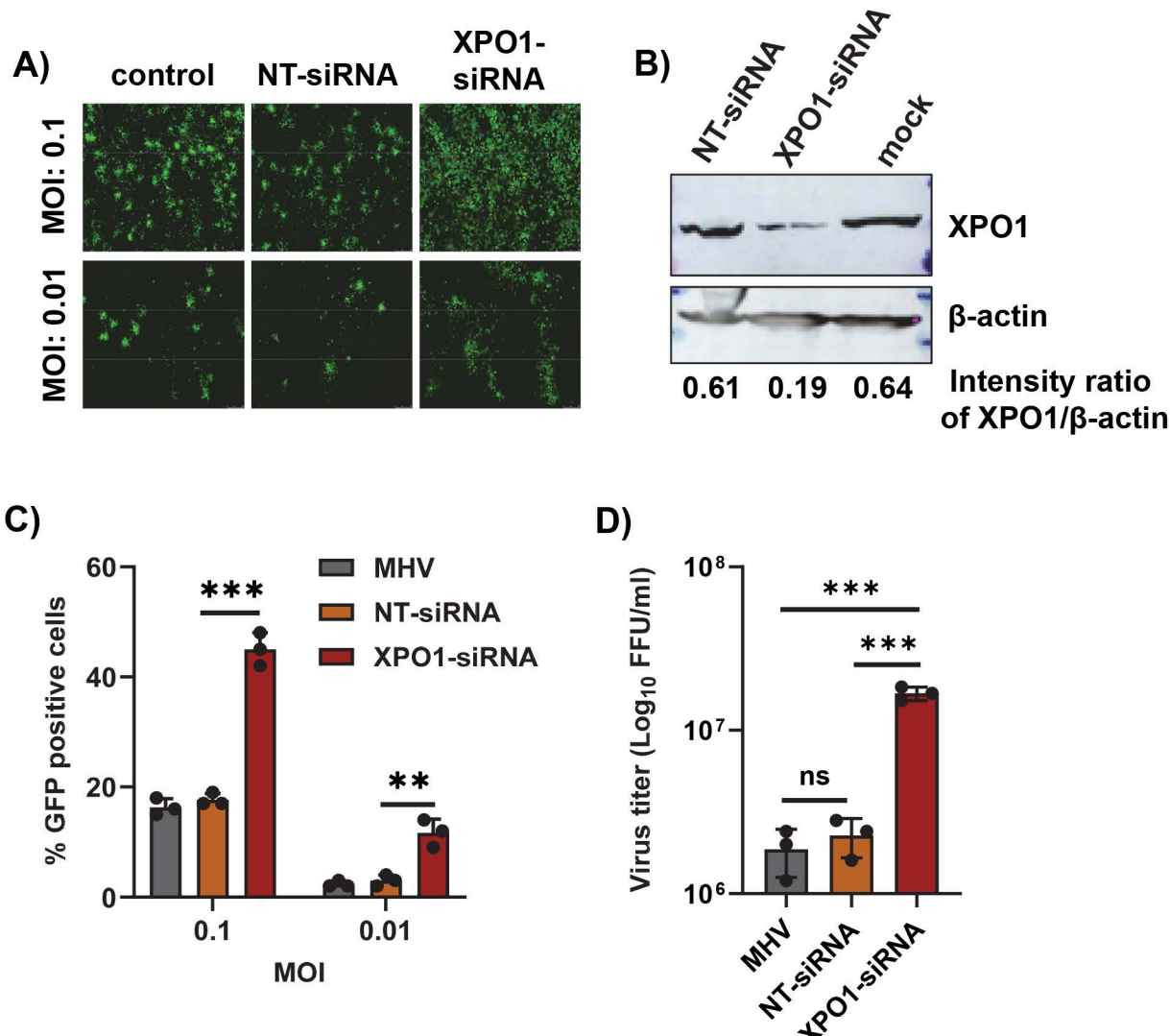
A)
control
NT-siRNA
XPO1-siRNA
MOI: 0.1
MOI: 0.01
B)
NT-siRNA
XPO1-siRNA
mock
XPO1
β-actin
0.61
0.19
0.64
Intensity ratio of XPO1/β-actin
C)
% GFP positive cells
60
40
20
0
***
**
MHV
NT-siRNA
XPO1-siRNA
0.1
0.01
MOI
D)
Virus titer (Log10 FFU/ml)
10^8
10^7
10^6
***
***
ns
MHV
NT-siRNA
XPO1-siRNA

Figure 6

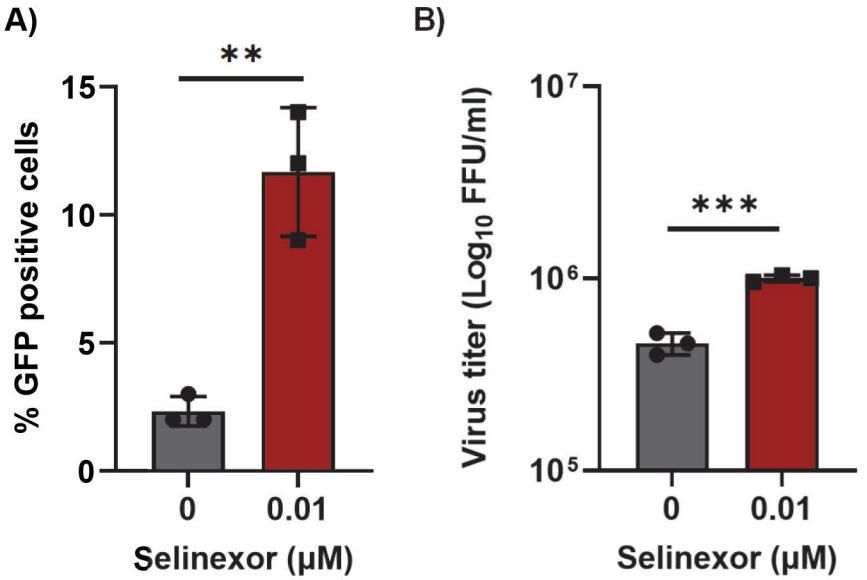
A)
**
15
10
5
0
% GFP positive cells
0
0.01
Selinexor (μM)
B)
***
10^7
10^6
10^5
Virus titer (Log_{10} FFU/ml)
0
0.01
Selinexor (μM)

Figure 7

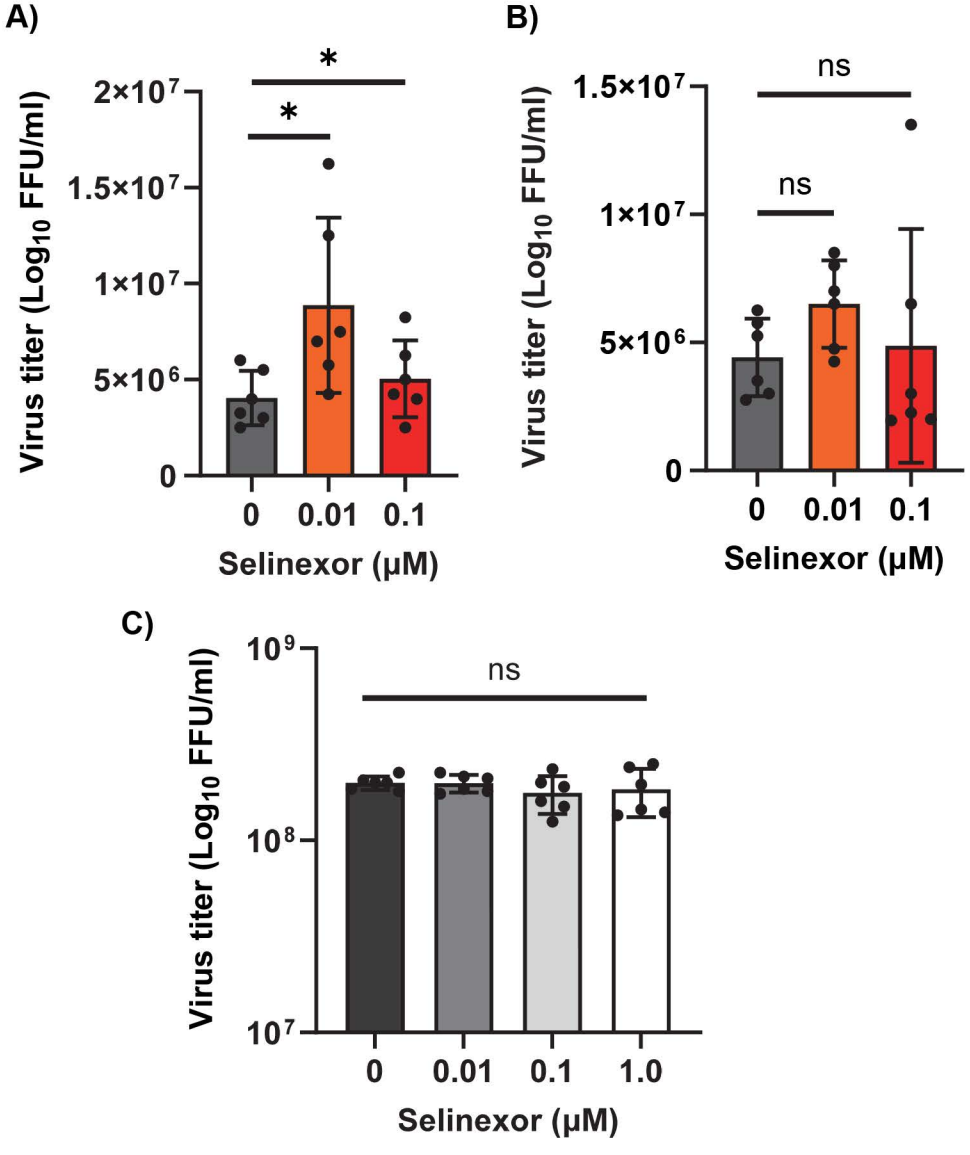
A)
B)
C)
Virus titer (Log10 FFU/ml)
2×10^7
1.5×10^7
1×10^7
5×10^6
0
*
*
ns
ns
10^9
10^8
10^7
0
0.01
0.1
1.0
Selinexor (μM)